International Journal of Innovative Computing, Information and Control
Volume **11**, Number **4**, August **2015**

ICIC International ©2015 ISSN 1349-4198
pp. 1357–1368

FEATURE QUALITY BASED SCORE LEVEL FUSION USING RELATIVE ENTROPY MEASURE FOR IRIS RECOGNITION

Norman Nelufule[1], Fulufhelo Nelwamondo[1,2], Tendani Malumedzha[1] and Tshilidzi Marwala[2]

[1]Modelling and Digital Science Unit
Council for Scientific and Industrial Research
Meiring Naude Road, Brummeria, Pretoria 0001, South Africa
{ nnelufule; fnelwamondo; tmalumedzha }@csir.co.za

[2]Department of Electrical and Electronics Engineering Sciences
University of Johannesburg
Auckland Park, Johannesburg 2006, South Africa
tmarwala@uj.ac.za

Received September 2014; revised February 2015

Abstract. *In this paper we propose an adaptive fusion approach for iris biometric. The proposed fusion method incorporates four matching algorithms using feature quality and relative entropy to enhance iris fusion performance. This method introduces relative entropy measure to the fusion process to assign low weighting coefficients to features with less information and higher weights to features with more information. We investigated the parameters which influence the rejection rates and acceptance rates to determine the optimal equal error rate. The best equal error rates were aimed at high recognition accuracy. The proposed method was tested on two public iris databases. CASIA left eye images produced 99.36% recognition accuracy and 0.041% equal error rate as compared to 98.93% recognition accuracy and 0.066% error rate produced by the weighted sum fusion. For the CASIA right eye images, the proposed method produced 99.18% recognition accuracy and 0.087% equal error rate as compared to weighted sum fusion with 98.81% recognition accuracy and 0.096% equal error rate. From the UBIRIS database, the proposed method produced 99.59% recognition accuracy and 0.038% equal error rate as compared to 98.53% recognition accuracy and 0.074% equal error rate produced by weighted sum fusion. The proposed method shows improved recognition performance in terms of AUC and the EER.*

Keywords: Score level fusion, Scores normalization, Weighted sum fusion, Simple sum fusion, Adaptive fusion, Relative entropy

1. **Introduction.** Fusion techniques have become the popular approach to enhance matching performance and recognition accuracy levels. This is because unimodal approaches are faced with many limitations which reduce recognition performance. Various levels of fusion approaches have been introduced to solve the recognition performance problem. These include multi-sensor fusion, multi-instance fusion, multi-sample fusion and multimodal fusion. The choice of level of fusion depends on the data available to use. In [1], Desoky *et al.* presented fusion results from template fusion. The challenge of using template fusion arises when different feature extraction methods produce incompatible features which may be of varying dimensions which suffer computational expense. To overcome this drawback, attention has been shifted on score based fusion. This is because scores acquisition is easy and scores provide more information about the templates being matched. Nandakumar *et al.* in [2] used a score based fusion approach using likelihood ratio-test density based estimation. Gaussian mixture model was used to model

the distribution of genuine and impostor scores in order to produce robust results using likelihood-based ratio-test estimation. This method requires the distribution of scores to be estimated accurately. If the distributions of scores have not been accurately estimated, this fusion method can produce undesirable results. Gawande *et al.* [3] implemented a multi-algorithmic fusion using three different iris feature extraction techniques. Wang *et al.* [4] also implemented similar procedure by combining phase information and zero crossings features using support vector machines. The use of multi-algorithmic fusion requires score normalization. He *et al.* [5] assessed the performance of score level fusion methods and their score normalization techniques in order to determine the more robust score normalization method. In their work they implemented simple sum rule fusion and compare them with support vector machine fusion approaches. Their results demonstrated that the latter can produce improved recognition performance if the kernel parameters have been carefully chosen. Kumar and Passi [6] also argued that the sum rule based offers added advantage of ease of computation as compared to learning based fusion approaches. On the contrary, Wang *et al.* [7] presented results tested using various fusion methods based on UBIRIS database and their results show that with highly accurate kernel parameters set, support vector machine outperforms simple sum fusion. With these current fusion methods, feature quality is not measured to enhance fusion performance. Measuring feature quality is useful in order to account for low quality features and high quality features during fusion. However, measuring feature quality for fusion is also a challenging task. This challenge motivated this work to introduce adaptive fusion which incorporates feature quality metrics and the error rates produced by each matcher. The metric for measuring the feature quality was based on the relative entropy measure which was also used in [8]. It is imperative to map feature quality values with the fusion function since quality improves system performance and increases system robustness. Our novelty lies in introducing the quality metric parameter and incorporating it with the EER during fusion. The significance of this contribution lies in improving recognition performance even on noisy iris images.

2. **Our Method.** Our fusion approach combines four matching algorithms, namely National Hamming Distance (NHD) [9-11], Weighted Hamming Distance (WHD) [12,13], Weighted Euclidean Distance (WED) [14] and Phase Only Correlation (POC) [15]. This fusion approach exploits the feature quality measure of each extracted feature from the feature extraction algorithms. The choice of algorithms was based on their efficiency in extracting iris information. Combination of these algorithms would indeed enhance iris recognition performance even on noisy iris images. In this work, each algorithm was implemented independently and assessed based on the effect of noise reduction using the EER measurements for each iris recognition method. The EER was computed from two related algorithms and used to compute the weighting parameters during fusion process. The procedure followed to accomplish the proposed approach is depicted in Figure 1. To get the features to assess their quality and the scores from each matcher we followed the procedure in [9-11] to preprocess raw data. The stages performed on preprocessing were segmentation and normalization.

2.1. **Iris image segmentation.** Iris image acquisition requires that the eye image should be captured with its surrounding parts which include parts of the face. Captured iris images are highly occluded with noise and the entire eye image is not necessary during subject's recognition. The region of interest should be segmented using efficient segmentation algorithms in order to isolate the iris region from other unwanted parts of the eye image. Accurate segmentation offers increased potential to enhance recognition

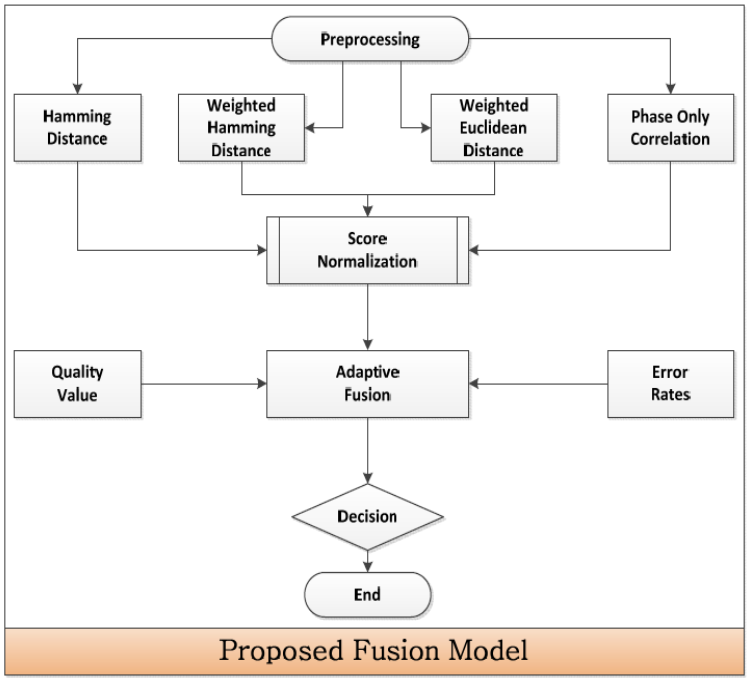

FIGURE 1. Structure of the proposed fusion

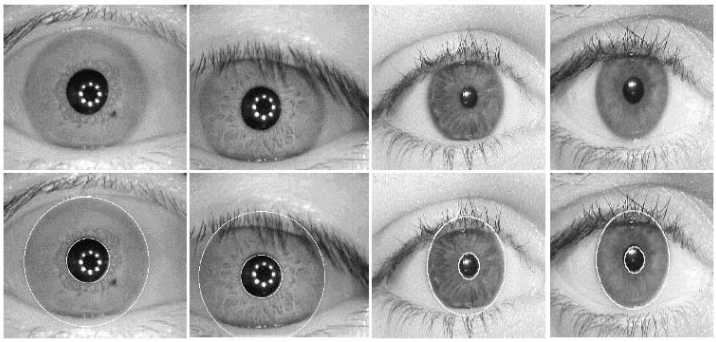

FIGURE 2. Segmentation results from CASIA and UBIRIS images

performance. Segmentation is the process of using robust algorithms to remove unnecessary parts of the eye image into a useful selected set of data which is transformed into mathematical measurements or model which represent the original image. In this work, an approach introduced by Masek in [16] was adopted and used to segment eye images. From the two databases used in this work, not all images were accurately segmented. Images with segmentation failures were discarded from test results to avoid their influence. The results of images which were accurately segmented are shown in Figure 2. The first row of Figure 2 shows raw images before segmentation and the last row shows the results of segmentation algorithm as implemented in this paper. The first two columns show images from CASIA iris database and the last two columns are images extracted from UBIRIS database.

Regardless of the success of segmentation, noise regions are the major causes of degraded iris recognition performance. The next step is to detect and remove noise using thresholding techniques. Detected noise regions such as eyelashes and eyelids are masked in order to exclude them during feature extraction. However, not every noise region

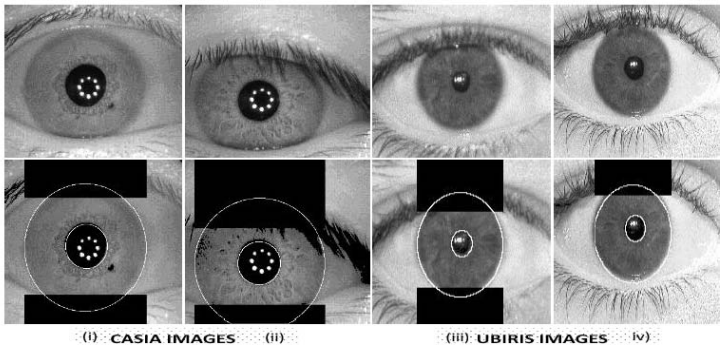

FIGURE 3. Results of noise masking for CASIA and UBIRIS images

within the image was able to be identified as noise region. The results of noise masking are presented in Figure 3.

The columns marked (i) through (iv) in Figure 3, depict noise masking on a segmented iris image. The masked regions include eyelashes, eyelids and specular reflection from the camera which can be seen from the image in the second row and first column. The images in the first two columns marked (i) and (ii) are from CASIA iris database; and columns marked (iii) and (iv) are from UBIRIS database.

2.2. **Iris image normalization.** To extract consistent features from all the images, segmented image should be normalized to correct for image deformation. In this work the Daugman Rubber sheet model [9-11] was adopted and used to normalize the iris region. This procedure involves mapping each image pixel from rectangular coordinate to polar coordinates. The reason for transforming the iris region into a normalized form is to gain consistency in image sizes and to avoid image deformations caused by the distance between the cameras and the subject, head tilt, pupil dilation, etc. Figure 4 shows the results of normalization method, with the segmented and masked images on the first column and their corresponding features and noise masks on the second column. The first two rows marked (i) are images from CASIA database and the last two rows marked (ii) are images from UBIRIS database.

Images in column two shows the results of pixels transformation from rectangular coordinates to polar coordinates using normalization algorithm. The arrow is showing the

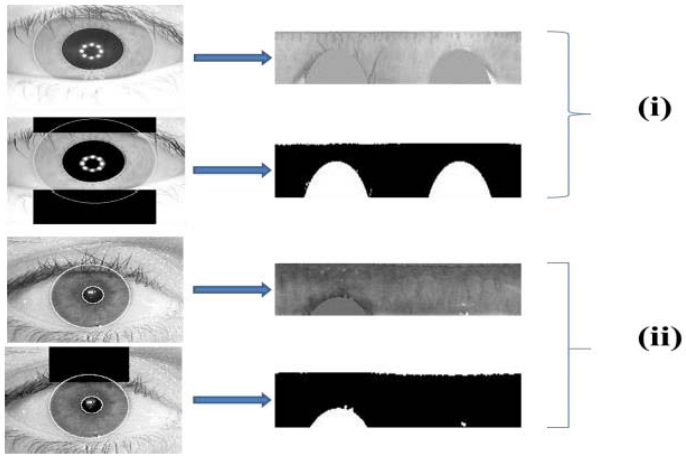

FIGURE 4. Results of normalization for CASIA and UBIRIS images

image before transformation and points to the image after transformation. The rectangular blocks of images showed in the second column are unwrapped iris images with iris features in gray and their corresponding noise masks in black and white. To assess feature quality, relative entropy was adopted and used to measure and generate the quality metrics for both intra and inter classes. The quality values were computed on extracted features because different feature extraction methods were used. The features were extracted from the blocks of images in the second column of Figure 4. It was imperative to assess and compute quality values on the extracted features in order to measure the amount of feature information and feature quality after extraction. The samples of extracted features assesses using relative entropy are shown in Figure 5.

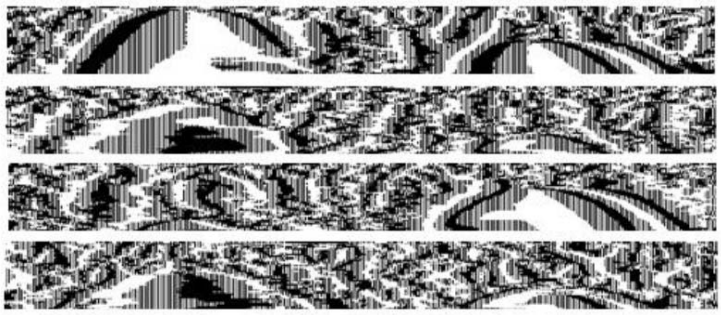

FIGURE 5. Samples of image features

2.3. **Iris feature extraction and feature matching.** Since the combination approach proposed here incorporates scores from four iris matching algorithms, features were extracted using four different extractors. The first set of features was extracted using Gabor filters at multiple scales. The feature comparison was done using the NHD. The procedure for this approach can be found in [9-11]. The second set of features was extracted using multi-lobe differential filters. To generate the scores, features were classified using WHD which uses adaptive weight maps to reduce the effect of noise during matching. Details of this approach can be found in [12,13]. The third set of features was extracted using the multi-channel Gabor filtering. Extracted features were classified using WED. The procedure for this approach can be found in [14]. The last set of features was extracted from blocks within the iris region using hierarchical models. Feature classification was done using POC. Since features were extracted using various approaches which extract different features, feature fusion would be very complex due to incompatibility challenges. Score level fusion was the most convenient because matching scores contain very useful explanation about the matching algorithms used. Due to the use of different matchers, scores also appear at a heterogeneous scale. To transform the matching scores to a homogeneous scale prior to fusion, the scores were converted to homogenous scales using hyperbolic tangent normalization in order to increase simplicity and compatibility during fusion.

2.4. **Feature quality measure.** Measuring feature quality offers an added advantage during classification. It is crucial to use consistent features to avoid an increase in *EER* due to inconsistent features extracted. The approach taken here differs from that in [17] which measures image quality by assigning a 1 for consistent bit and 0 otherwise. The proposed approach of measuring feature quality was adopted from [8], where relative entropy was used. The relative entropy, also known as Kullback Leibler Divergence (KLD) measures the difference between non-symmetric probability distributions. KLD has received considerable attention in information theory and its application in image quality

assessment remains crucial. Variations in feature distribution need to be quantized in a biometric systems seeking robustness. *KLD* is a good measure of variations between two probability distributions. Generally the *KLD* may be expressed mathematically in terms of Equation (1).

$$KLD(z||w) = \int_x z(x) \log_2 \left(\frac{z(x)}{w(x)} \right) \tag{1}$$

This metric is very useful in measuring information loss if the parameter w is used to estimate z as described by Equation (1). According to Equation (1), the functions $z(x)$ and $w(x)$ are the probability mass functions of the intra-class and inter-class distribution respectively; and whose integrals can be computed along the feature vector space, X. Since *KLD* measures the expected amount of extra information required to encode one distribution of set of features to another distribution, the feature mean intensity becomes necessary. For each class of probability distribution, the mean intensity for each normalized image can be computed using Equations (2) and (3) as explained below.

$$E_z(x) = \frac{1}{N} \sum_{i=1}^{N_z} X_i \tag{2}$$

The parameter E_z in Equation (2) represents an expected value of the probability distribution function, $z(x)$.

$$E_w(x) = \frac{1}{N} \sum_{i=1}^{N_w} X_i \tag{3}$$

The parameter E_w in Equation (3) represents an expected value of the probability distribution function, $w(x)$. The covariance of the probability mass functions $z(x)$ and $w(x)$ were computed using Equations (4) and (5).

$$\sum_z = \left[(X - E_z)^t (X - E_w) \right] \tag{4}$$

$$\sum_w = \left[(X - E_w)^t (X - E_z) \right] \tag{5}$$

The probability mass functions $z(x)$ and $w(x)$ can now be transformed into Equations (6) and (7) by combining Equations (4) and (5).

$$z(x) = \frac{1}{\sqrt{|2\pi E_z|}} . \exp \left(-\frac{1}{2} (X - E_z)^t \sum_z^{-1} (X - E_z) \right) \tag{6}$$

$$w(x) = \frac{1}{\sqrt{|2\pi E_w|}} . \exp \left(-\frac{1}{2} (X - E_w)^t \sum_w^{-1} (X - E_w) \right) \tag{7}$$

The relative entropy measure which was used to measure the quality of the feature distribution of the intra-class $z(x)$ and inter-class $w(x)$ was computed using Equation (8). This procedure can also be found detailed in [8].

$$KLD(z||w) = \int z(x) \left(\log_2 z(x) - \log_2 w(x) \right) dx \tag{8}$$

The values computed by Equation (8) range between 0 and 1. The relative entropy values were ranked prior to fusion, and Table 1 shows the rankings.

TABLE 1. Table of KLD value ranking

Rankings	**Min(KLD)**	**Max(KLD)**
High	0.90	1.00
Good	0.59	0.89
Low	0.39	0.58

2.5. **Score normalization and fusion.** Matching scores were generated from various algorithms which output heterogeneous scores. In this work, the scores generated from NHD, WHD and POC were homogeneous and ranging from *(0-1)*. The scores generated from WED were at a scale of *(0-100)*. To alleviate this anomaly, we normalized the matching scores prior to fusion to ensure homogeneity using the hyperbolic tangent estimator normalization. The hyperbolic tangent was adopted to transform the matching scores to a *(0-1)* homogeneous scale for fusion compatibility due to its robustness and efficiency against score which may appear as outliers. The hyperbolic tangent can be expressed mathematically in terms of Equation (9).

$$S_{Norm} = \left\{ \frac{1}{2} \left(\tanh \left(0.01 \left(\frac{S_i - \bar{S}}{\sigma} \right) \right) \right) + 1 \right\} \tag{9}$$

The parameter S_{Norm} is an output of the normalized scores, S_i is the raw scores data before normalization, $\bar{S}$ is the mean of the raw scores and σ is the standard deviation of the raw scores. The value 0.01 represents the spread of the scores distribution. The parameter $\bar{S}$ which is an estimated mean of the raw genuine scores was estimated using Hampel estimating parameters [18] which are computed using the influence function in Equation (10).

$$h(y) = \begin{cases} y & 0 \leq |y| < a \\ a * sign(y) & a \leq |y| < b \\ a * sign(y) * \left(\frac{c-|y|}{c-b} \right) & b \leq |y| < c \\ 0 & |y| \geq c \end{cases} \tag{10}$$

In Equation (10) the parameter y denotes the value of the genuine scores which is the difference between the genuine score distribution and the median value of the genuine scores. The value of $\bar{S}$ is obtained as a result of the sum of the median value and the output of the influence function, $h(y)$. This normalization algorithm is very robust to outliers but its optimality depends mainly on the parameters a, b and c which should be chosen with much caution. The choice of these three parameters was based on the tuple α, β and γ. In our case, the choice $\alpha = 80$, $\beta = 90$ and $\gamma = 95$ produced the highest recognition performance in terms of the Area Under the Curve (AUC) and the EER. From this tuple, the parameters (a, b, c) were chosen in such a way that $\alpha\%$ of the genuine scores should at least fall within the range $(m - a, m + a)$, $\beta\%$ of all the genuine scores should at least fall within the range $(m - b, m + b)$ and $\gamma\%$ of all the genuine scores should at least fall within the range $(m - c, m + c)$, where the parameters a, b and c are as they appear in Equation (10) which estimate the influence function.

Our main results are reported using the Receiver Operating Characteristic (ROC) curve and tables which show the values of the AUC and EER in Section 3. The final matching decision was also determined to render a match or a mismatch. This decision was based on a predefined threshold value which offers increased performance. The decision threshold method for a match or a mismatch was defined using Equation (11).

$$D = \begin{cases} A, & T_S \leq S_i \\ R, & \text{Otherwise} \end{cases} \tag{11}$$

The decision module accepts a biometric user if the submitted biometric returns a match score which is lower or equal to the predefined threshold. If the return result is otherwise, the biometric system will recognize a user as an impostor and rejects the biometric user. In Equation (11), D is the decision module parameter after comparison, A is the accept decision, R is the reject decision, T_S is the predefined threshold from the fused scores and S is a vector of all the individual scores.

3. **Results and Discussions.** Results presented here were derived from two public iris databases, namely CASIA-IrisV3-Interval and UBIRIS datasets. From the CASIA database we used the left and right eye images separately and compared their results on various figures. We selected *275* left eye images from CASIA and *815* from right eye images. They were all saved as *320×280 JPEG* image files. The images selected were from different subjects because we used five instances for each subjects and some subjects had less than the desired number of instances. We selected *1200* right eye images from UBIRIS database whose description says they were captured at *300* dpi and saved as *2560×1704 JPEG* image files. The training sets reported here are images which were segmented correctly so that segmentation failure will not pose bias of our fusion results. Results from each matching algorithm were analyzed using various threshold values before fusion. The EERs for each matcher were calculated to determine the individual performance of each matcher. Table 2 below shows the performance of individual matchers using false rejection rates at a constant false accepts rate. These errors were incorporated in the fusion process together with the quality values to compute the fusion weights. From the false rejection rates shown below at equal false accepts rate assigned at zero level, the varying levels of recognition performance can be easily determined.

TABLE 2. Table of error rates from individual matchers

Algorithm	**FAR (%)**	**FRR (%)**
Gabor Filter	*0.00*	*0.0082*
Multi-Channel Gabor Filter	*0.00*	*0.0086*
Multi-Lobe Differential Filter	*0.00*	*0.0063*
Hierarchical Phase Based	*0.00*	*0.0065*

During the fusion process, various weights were investigated and the optimal combination which results to low error rates was selected. Various fusion approaches were implemented, investigated and compared with the proposed fusion model. The proposed fusion approach outperformed all other traditional fusion approaches when tested against all the datasets. The performances of these algorithms were tested using the AUC and EER. The ROC curves are also presented which show all the fusion techniques tested on all three datasets. Table of performance measures appear after each ROC curve. When the distinction between impostor scores and the genuine scores is high, the system security increases and error rates also decline due to high distinction between the two score distribution. However, when the distinction between the impostors and the genuine scores is very low, it becomes difficult to set an effective optimal threshold value and these lead to impostors gaining access or genuine users being denied of access. System security becomes very poor and error rates also increase. In this work it was discovered that the performance of the fusion algorithm is highly influenced by the quality parameters and the weighting coefficients computed from the EER of individual matcher shown in Table 2. Our experimental results tested against the CASIA left eye images are presented in figure below.

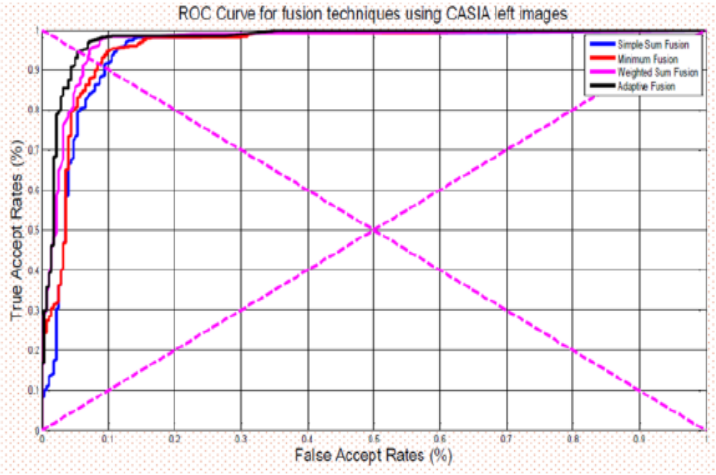

FIGURE 6. ROC curve for CASIA left eye images

From the ROC Figures 6 and 7 it shows that the CASIA left eye images performs better than the CASIA right images. However, the images used in this work have been extracted from various subjects, due to the condition of five instances desired for each image. Since various subjects were used in the CASIA database, the results from Figure 6 and Figure 7 cannot significantly deduce that the left eyes are better than the right eyes. From the images used in both left and right eye images, resolutions vary and the level of noise between them also vary. For these databases results were highly influenced by the weighting parameters used, since they were not adjusted to suit a specific database during matching. The weights incorporated in the adaptive fusion process were *(0.4, 0.6)* and *(0.6, 0.4)* which produced the best results in terms of low EER and high AUC. For the weighted sum the best results were achieved with weight of *(0.3, 0.7)* and *(0.7, 0.3)* when fusing the four scores from four iris matching algorithms. Table 3 below shows the results of comparison of other sum rule based fusion techniques against the proposed adaptive fusion. From this table of results, the proposed adaptive fusion has high accuracy as shown by the value of AUC and improved performance as shown by its low EER.

TABLE 3. Table of performance and EER for CASIA left eye images

Fusion Algorithm	**Performance (%)**	**EER (%)**
Sum Fusion	*98.3*	*0.0092*
Minimum Fusion	*98.6*	*0.074*
Weighted Sum Fusion	*98.9*	*0.066*
Proposed Fusion	*99.3*	*0.041*

Table 4 demonstrates the performance of the proposed approach as compared against the other fusion approaches using the CASIA right eye images. The table shows that the proposed method outperforms the other fusion approaches both in terms of AUC and EER values.

Table 5 shows performance of the proposed fusion against other fusion approaches using the UBIRIS database. The UBIRIS as shown by Table 5 and ROC curve shown in Figure 8 outperforms all the databases tested. The proposed method produces excellent results even on the noisy iris database when noise parameters are accounted for during the fusion process. This is evident from the results of our approach compared to the results produced by the state-of-the art fusion methods.

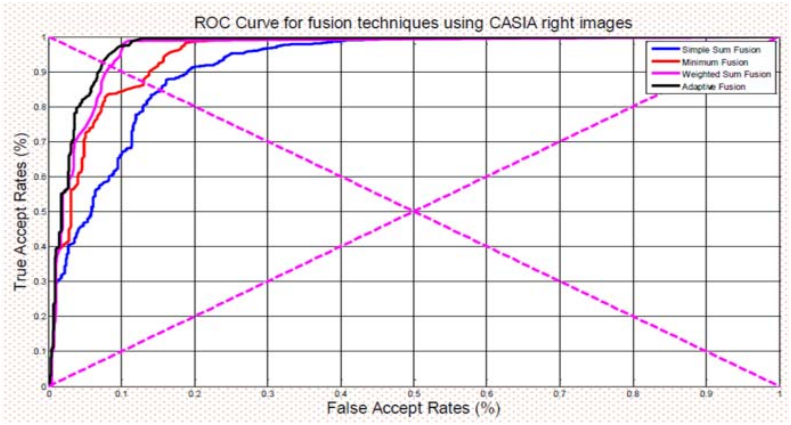

FIGURE 7. ROC curve for CASIA right eye images

TABLE 4. Table of performance and EER for CASIA right eye images

Fusion Algorithm	Performance (%)	EER (%)
Sum Fusion	*97.0*	*0.17*
Minimum Fusion	*98.4*	*0.12*
Weighted Sum Fusion	*98.8*	*0.096*
Proposed Fusion	*99.1*	*0.087*

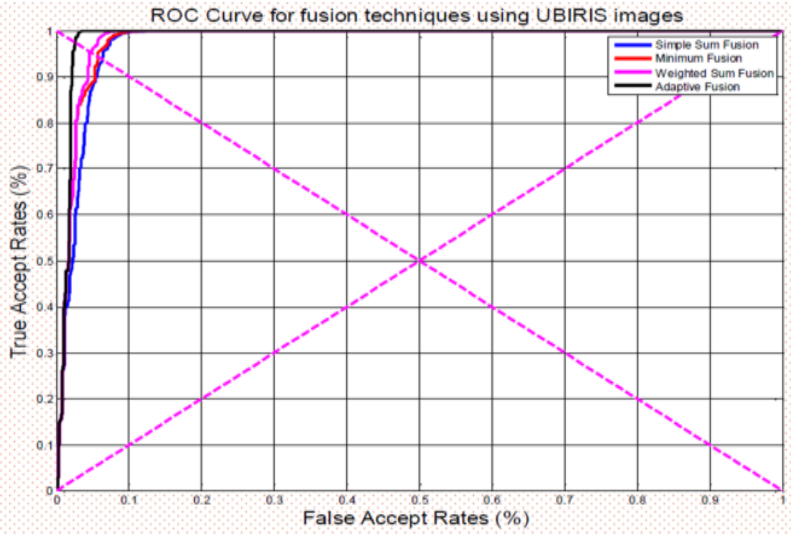

FIGURE 8. ROC curve for UBIRIS images

TABLE 5. Table of performance and EER for UBIRIS images

Fusion Algorithm	Performance (%)	EER (%)
Sum Fusion	*97.0*	*0.17*
Minimum Fusion	*98.26*	*0.0069*
Weighted Sum Fusion	*98.53*	*0.074*
Proposed Fusion	*99.59*	*0.038*

4. **Conclusions.** An adaptive quality based fusion approach based on the weighted minimum score fusion has been proposed and presented. The experimental results for the proposed quality based fusion approach were tested against CAISA and UBIRIS iris images databases. The results presented using ROC demonstrates that an adaptive fusion method with tuned weights performs better than a weighted fusion approach. Evidence from the two datasets demonstrated that recognition performance increases when quality values are incorporated during fusion. A large dataset from a noisy database also demonstrated the capability. From the tables and ROC figures it is clear that the adaptive fusion outperforms the weighted sum fusion and the other state-of-the-art fusion methods by a significant gap. In all the training datasets the proposed approach produced low EER rates and high AUC which determines the recognition performance and biometric system accuracy. The left eye images from CASIA gave better recognition accuracy over its right eye images. Nevertheless, the images used were taken from various subjects whose images were taken on different sessions. This is because most of the image files are missing on CASIA-IrisV3-Interval database, and for this work five training images per subject were used. The type of training images in terms of pixels resolutions differs based on the imaging conditions of different sessions. It was also noted that various subjects possess varying levels of eyelashes which also include hiding the iris region with their eyelids. Most training images used from left eye were highly rich in iris features as compared to the training images from the right eye. These features have led to better recognition of left eyes over right eyes. In future, this work will be extended to assessing feature quality values by dividing the image into blocks and measure the quality of features from each block. This will improve the recognition performance and system accuracy even more.

Acknowledgment. The authors wish to thank the Department of Science and Technology (DST) of South Africa and the Council for Scientific and Industrial Research (CSIR) for their funding contributions on this research work.

REFERENCES

[1] A. I. Desoky, H. A. Ali and N. B. Abdel-Hamid, Enhancing iris recognition system performance using templates fusion, *Ain Shams Engineering Journal*, vol.3, no.2, pp.133-140, 2012.

[2] K. Nandakumar, Y. Chen, S. C. Dass and A. K. Jain, Likelihood ratio-based biometric score fusion, *IEEE Trans. Pattern Analysis and Machine Intelligence*, vol.30, no.2, pp.342-347, 2008.

[3] U. Gawande, M. Zaveri and A. Kapur, Improving iris recognition accuracy by score based fusion method, *International Journal of Advancements in Technology*, 2010.

[4] F. Wang, J. Han and X. Yao, Iris recognition based on multi algorithmic fusion, *WSEAS Trans. Information Science & Applications*, vol.12, no.4, pp.1415-1421, 2007.

[5] M. He, S. Horng, P. Fan, R. Run, R. Chen, J. Lai, M. K. Khan and K. O. Sentosa, Performance evaluation of score level fusion in multimodal, *Pattern Recognition*, vol.43, pp.1789-1800, 2010.

[6] A. Kumar and A. Passi, Comparison and combination of iris matchers for reliable personal authentication, *Pattern Recognition*, vol.43, no.3, pp.1016-1026, 2010.

[7] F. Wang, X. Yao and J. Han, Minimax probability machine multialgorithmic fusion for iris recognition, *Journal of Information Technology*, vol.6, no.7, pp.1043-1049, 2007.

[8] R. Youmaran and A. Adler, Measuring biometric sample quality in terms of biometric, *Journal of Electrical and Computer Engineering*, vol.2012, p.9, 2012.

[9] J. Daugman, High confidence visual recognition of persons by a test of statistical independence, *IEEE Trans. Pattern Analysis and Machine Intelligence*, Cambridge, 1993.

[10] J. Daugman, How iris recognition works, *IEEE Trans. Circuits and Systems for Video Technology*, 2004.

[11] J. Daugman, The importance of being random: Statistical principles of iris recognition, *The Journal of Pattern Recognition Society*, pp.279-291, 2003.

[12] W. Dong, Z. Sun and T. Tan, Iris matching based on personalized weight map, *IEEE Trans. Pattern Analysis and Machine Learning*, 2011.

[13] Z. Sun and T. Tan, Ordinal measures for iris recognition, *IEEE Trans. Pattern Analysis and Machine Intelligence*, 2009.

[14] T. Tan, Texture feature extraction via visual cortical channel modelling, *Proc. of IEEE International Conference on Pattern Recognition*, pp.607-610, 1992.

[15] D. Durai and M. Karnan, Iris recognition using modified hierarchical phase-based matching technique, *International Journal of Computer Science Issues*, vol.7, no.8, pp.43-48, 2010.

[16] L. Masek, *Recognition of Human Iris Patterns for Biometric Identification*, Ph.D. Thesis, University of Western Australia, 2003.

[17] H. Proenca and L. Alexandre, Iris recognition: Measuring feature's quality for the feature selection in unconstrained image capture environments, *IEEE Proc. of the 2006 International Conference on Computational Intelligence for Homeland Security and Personal Safety*, Alexandria, 2006.

[18] F. R. Hampel, E. M. Ronchetti, P. J. Rousseeuw and W. A. Stahel, *Robust Statistics: The Approach Based on Influence Functions*, Vol.114, John Wiley & Sons, 2011.